



---

## Study on the Mechanism of the Effects of Coal Particles on the Mechanical Properties of Cement-Based Grouting Materials

Chen Feng

School of Safety Science and Engineering, Henan Polytechnic University, Jiaozuo Henan 454000, China  
Email : 19511987556@163.com

---

**Abstract** This paper systematically investigates the effects of coal particle content and size on the macroscopic mechanical properties and microstructure of cement-based grouting materials, with the goal of improving the sealing performance of gas extraction boreholes. A series of experiments with varying coal particle contents and sizes were conducted to measure the compressive strength at different curing ages. Additionally, Scanning Electron Microscopy (SEM) and X-ray Diffraction (XRD) were employed to analyze the microstructure and hydration products of the materials. The results demonstrate that the incorporation of an optimal amount of coal particles significantly enhances the mechanical properties of cement-based materials, with a content of 40g and a particle size of 1–2mm achieving the highest compressive strength. Microstructural analysis revealed that the appropriate introduction of coal particles promotes the formation of C-S-H gel, thereby improving material compactness and durability. This research provides crucial theoretical insights and practical guidance for the application of cement-based grouting materials in gas extraction operations.

**Keywords** coal particles; cement-based grouting material; compressive strength; microstructure; gas extraction

---

### 1. Introduction

Coal remains a fundamental industrial raw material and the most essential energy source in China, offering a secure and economically viable means for clean and efficient utilization. As the primary energy resource and a critical industrial feedstock, coal plays a vital role in supporting the nation's economic growth and ensuring energy security and stable supply<sup>[1,2]</sup>. Coalbed methane (CBM), a type of unconventional natural gas primarily composed of methane adsorbed onto the surface of coal matrix particles, is a key byproduct of coal formation. It is estimated that China possesses coalbed methane reserves of approximately  $36.81 \times 10^{12} \text{ m}^3$  at depths shallower than 2000 meters, of which  $10.87 \times 10^{12} \text{ m}^3$  (about 30%) is recoverable<sup>[3,4]</sup>. However, CBM is also a major hazard in coal mines, being a significant factor in gas explosions, coal and gas outbursts, and gas combustion accidents. From 2008 to 2020, gas-related accidents accounted for 33% of the total fatalities in coal mining, surpassing other major causes such as roof collapses, water disasters, and mechanical failures<sup>[5,6]</sup>. The persistent threat of coalbed methane hazards severely constrains the sustainable and safe development of the coal industry<sup>[7]</sup>. Effective CBM extraction not only ensures the safe operation of underground coal mining, improving worker productivity and mine efficiency, but also reduces greenhouse gas emissions and provides a clean energy source with significant economic benefits<sup>[8]</sup>. Gas extraction boreholes, capable of advanced, regional, and precise CBM drainage, are a critical technological solution for mitigating gas-related hazards<sup>[9]</sup>. However, the CBM extraction rate and concentration in many Chinese coal mines remain suboptimal. In addition to insufficient preliminary geological work and improper extraction methods, poor borehole sealing is a significant factor affecting the overall efficiency of CBM drainage. The quality of borehole sealing is crucial for enhancing the effectiveness of gas extraction. Properly selected grouting materials can effectively seal boreholes



and reinforce the gas extraction system, thereby improving extraction efficiency. With the continuous advancement of grouting technologies, the range and performance of grouting materials have seen substantial improvement. In Chinese coal mines, commonly used grouting materials fall into three categories: clay-based materials, polymer materials, and cement-based materials. Clay-based materials are fine, plastic mixtures of semi-dry clay, yellow mud, cement, or yellow mud-cement composites [10]. Polyurethane materials, known for their excellent performance, consist of two components—black material (polyether polyols, foaming agents, catalysts, etc.) and white material (isocyanates)—which form a foam upon mixing [11, 12]. Cement-based materials, the most widely applied grouting materials, are advantageous due to their adaptability to various geological conditions, adjustable fluidity and setting times, and the ability to ensure adequate borehole sealing lengths. Furthermore, industrial waste can be incorporated into cement-based formulations to create composite materials, lowering sealing costs [13].

Drilling operations generate a significant amount of coal particles, or coal cuttings, which not only occupy limited working space but also increase the ventilation resistance of roadways, and in severe cases, may lead to coal dust explosions, posing a serious threat to worker safety [14]. Studies have shown that in boreholes drilled at depths between 25 and 79 meters, the particle size of cuttings smaller than 2mm accounts for 89.88% to 92.68% of the total sample, with an average of 91.21% [15]. Based on this, the present study selects coal particles smaller than 2mm as a filler to be incorporated into a self-developed cement-based grouting material. The study explores the influence of different coal particle contents and sizes on the mechanical properties of the cement-based grouting material from both macroscopic and microscopic perspectives, with the aim of reducing costs while enhancing the mechanical performance of the grouting material.

## 2. Experiment

### Raw Materials

**Material Selection:** The silicate cement (PC) used in this study was P·O 42.5 cement produced by Jiaozuo Qianye Cement Co., Ltd. The sulfoaluminate cement clinker (SAC) was sourced from Jiaozuo Huayan Industrial Co., Ltd., specifically a rapid-hardening (low alkalinity) sulfoaluminate cement. The chemical compositions of these two types of cement are presented in Table 1. Gypsum was procured from the Daan Gypsum Plant in Quxian County, Shanxi Province. The early strength agent utilized was a calcium formate early strength agent produced by Shandong Chemical Factory. The suspending agent employed was sodium-based bentonite developed by Jianping Hengtong Mining Co., Ltd. Sodium carbonate, of analytical purity, was obtained from the Hongyan Reagent Factory in Hedong District, Tianjin. Coal samples were collected from the Jiulishan Mine of the Henan Coal Industry and Chemical Group, specifically of the anthracite type. The elemental and industrial analyses of the coal samples are detailed in Table 2.

**Table 1:** Chemical Composition of Cement

Cement	CaO	SiO <sub>2</sub>	Al <sub>2</sub> O <sub>3</sub>	Fe <sub>2</sub> O <sub>3</sub>	SO <sub>3</sub>	MgO	Na <sub>2</sub> O	K <sub>2</sub> O	TiO <sub>2</sub>
PC	61.67	21.75	5.57	3.58	2.36	2.21	0.43	0.87	0.00
SAC	40.23	6.36	38.27	1.27	8.88	1.15	0.00	0.00	1.77

**Table 2:** Elemental and Industrial Analysis of Coal Samples

Elemental Analysis		Industrial Analysis	
Element	Content /%	Composition	Content /%
C <sub>daf</sub>	88.78	M <sub>ad</sub>	7.08
H <sub>daf</sub>	1.81	A <sub>d</sub>	11.54
N <sub>daf</sub>	1.09	V <sub>daf</sub>	2.46
O <sub>daf</sub>	8.09	FC <sub>ad</sub>	78.95

### Sample Preparation and Testing Methods

The cement-based grouting materials used in this experiment were prepared by mixing silicate cement, sulfoaluminate cement, gypsum, sodium-based bentonite, and sodium carbonate in specific proportions. To investigate the effect of coal dust content on the mechanical properties of the cement-based grouting materials, coal dust was first sieved using a screen with an aperture diameter of 2 mm. Keeping the amount of the cement-



based grouting material constant, five groups of experiments were designed by varying the coal dust content, labeled as A1, A2, A3, A4, and A5. The composition ratios for each experimental group are presented in Table 3. Compressive strength was used as the evaluation index to determine the optimal coal dust content. At the optimal coal dust content, coal dust with particle size ranges of 1–2 mm (I), 0.5–1 mm (II), 0.25–0.5 mm (III), 0.075–0.25 mm (IV), and less than 0.075 mm (V) was selected for testing, labeled as B1, B2, B3, B4, and B5, respectively. The composition ratios for these experimental groups are shown in Table 4. Standard samples were prepared as illustrated in Figure 1.

**Table 3:** Composition Ratios of Different Coal Dust Additions

	PC/SAC	Coal Dust	Other Additives	H <sub>2</sub> O
A1	150	0	26	105.6
A2	150	20	26	117.6
A3	150	40	26	129.6
A4	150	60	26	141.6
A5	150	80	26	153.6

**Table 4:** Composition Ratios of Different Coal Dust Particle Sizes

	PC/SAC	Coal Dust	Other Additives	H <sub>2</sub> O
B1	150	40 (I)	26	129.6
B2	150	40 (II)	26	129.6
B3	150	40 (III)	26	129.6
B4	150	40 (IV)	26	129.6
B5	150	40 (V)	26	129.6

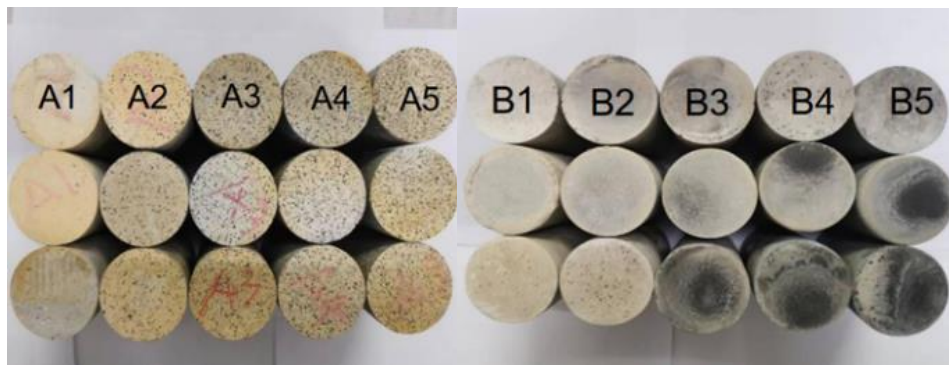


**Figure 1:** Diagram of Standard Specimens

Under standard curing conditions, uniaxial compression tests were conducted on the prepared standard specimens using the RMT-150B rock mechanics testing system produced by Wuhan Geotechnical Mechanics Institute. This system measured all mechanical parameters of the specimens. The surface micro-morphology of the materials was observed using a scanning electron microscope (SEM). The microstructural analysis was performed with the Quanta FEG 250 field emission environmental scanning electron microscope produced by FEI, USA. Qualitative and semi-quantitative analyses of the materials were carried out using an X-ray diffractometer, specifically the Smart Lab rotating target X-ray diffractometer produced by Japan's Rigaku Corporation, to analyze the phase composition of the hydration products in the coal dust-modified cement-based grouting materials.

### 3. Results and Discussion

#### Effect of Coal Dust Content on the Mechanical Properties of Cement-Based Grouting Materials

The compressive strength of the grouting materials is a crucial indicator of their load-bearing capacity. Figure 2 shows the results of uniaxial compressive strength tests for cement-based grouting materials at different coal



dust contents after 7 and 28 days of curing, with the average values obtained from three samples for each experimental group.

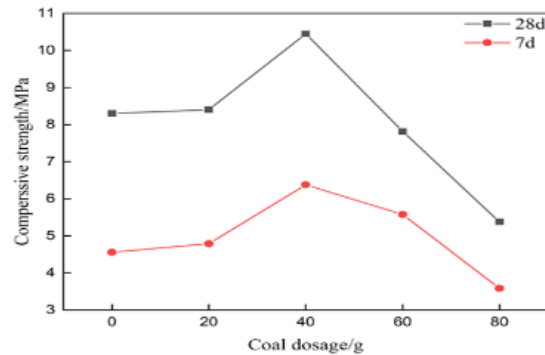


**Figure 2:** Uniaxial Compressive Strength of Cement-Based Grouting Materials at Different Coal Dust Contents

From Figure 2, it is evident that the compressive strength of samples A1 to A5 increases with the curing age. Notably, for sample A1, which has a coal dust content of 0%, the compressive strength shows the greatest increase from 7 days to 28 days, rising by 82.2%. In contrast, samples A2, A3, and A5 exhibit relatively smaller increases of 75.4%, 63.9%, and 50.0%, respectively, while sample A4 shows the smallest increase of only 40.2%. At the same curing age, the compressive strength of the samples initially increases with coal dust content but then decreases. At 7 days of curing, the compressive strengths of samples A2, A3, and A4 increase by 5.10%, 39.94%, and 23.39%, respectively, whereas sample A5 experiences a decrease of 21.37%. At 28 days of curing, the compressive strengths of samples A2 and A3 increase by 1.20% and 25.88%, respectively, while samples A4 and A5 decrease by 5.86% and 35.24%. This behavior can be attributed to the formation of a new skeletal structure within the cement matrix due to the addition of coal dust. Within a certain range, increasing the coal dust content enhances the density of the material, which, in turn, raises the compressive strength of the cement-based grouting materials. However, if the coal dust content is excessive, the distance between coal particles decreases, making it difficult for the cement matrix to effectively fill the voids between the coal particles and transmit stress. This can lead to defects within the material, resulting in reduced compressive strength. Furthermore, coal dust has significantly lower hydration activity compared to cement clinker; an excessive amount of coal dust reduces the proportion of cement clinker minerals in the system, slows down the hydration rate, and decreases the quantity of hydration products formed, thereby reducing strength. As seen in Figure 2, regardless of whether the curing period is 7 days or 28 days, the compressive strength of the cement-based grouting material reaches its peak when the coal dust content is 40 g (sample A3). Therefore, the optimal coal dust content is determined to be 40 g.

### Effect of Coal Dust Particle Size on the Mechanical Properties of Cement-Based Grouting Materials

From section 3.1, it is evident that a coal dust content of 40 g maximally enhances the compressive strength of the cement-based grouting materials. Therefore, while keeping the coal dust content constant, five different particle sizes were selected to study the impact of individual particle sizes on the mechanical properties of the cement-based grouting materials.

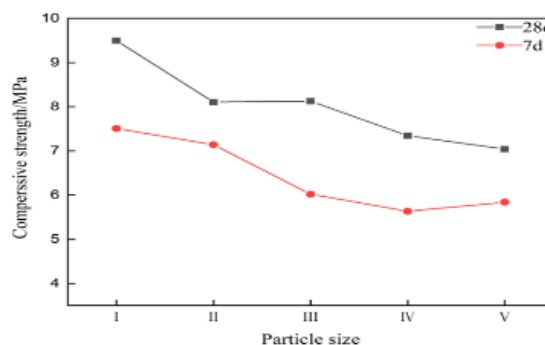


**Figure 3:** Uniaxial Compressive Strength of Cement-Based Grouting Materials at Different Coal Dust Particle Sizes



From Figure 3, it is evident that the compressive strength of samples B1 to B5 increases with the curing age. Among these, sample B3 exhibits the greatest increase in compressive strength from 7 days to 28 days, rising by 35.0%. In contrast, samples B1, B4, and B5 show relatively smaller increases of 26.6%, 30.4%, and 20.6%, respectively, while sample B2 shows the smallest increase at only 13.5%. At the same curing age, the compressive strength of the samples generally decreases as the particle size of the coal dust decreases. After 7 days of curing, the compressive strengths of samples B2, B3, B4, and B5 decrease by 4.8%, 19.8%, 24.9%, and 22.2%, respectively. At 28 days of curing, the compressive strengths of samples B2, B3, B4, and B5 decrease by 14.7%, 14.4%, 22.7%, and 25.9%, respectively. This trend can be attributed to the hydrophobic nature of coal. Smaller coal dust particles tend to distribute unevenly within the slurry. When the content of fine particles increases beyond a certain percentage, these smaller particles are more prone to agglomeration, resulting in reduced packing density and the formation of voids and weak areas in the microstructure of the consolidated material. Additionally, finer coal particles may cover the surfaces of cement particles rather than filling the voids within the consolidated body, leading to a reduction in hydration reactions and, consequently, a decrease in compressive strength. Under the same dosage, larger coal dust particles are fewer in number and can distribute more uniformly within the slurry compared to smaller particles, preventing agglomeration effects. Incorporating larger coal particles into the cement-based material can create a mixture with more nucleation centers than the original cement, and due to the absence of agglomeration effects, the larger coal dust exhibits a higher packing density [16], thereby increasing the compressive strength of the cement-based materials.

#### Scanning Electron Microscopy (SEM) Results

Based on the analysis above, it is clear that different dosages and particle sizes of coal dust significantly affect the mechanical properties of cement-based materials. Figures 6(a–f) present the SEM images of samples A3 and B1 to B5 after 28 days of curing.

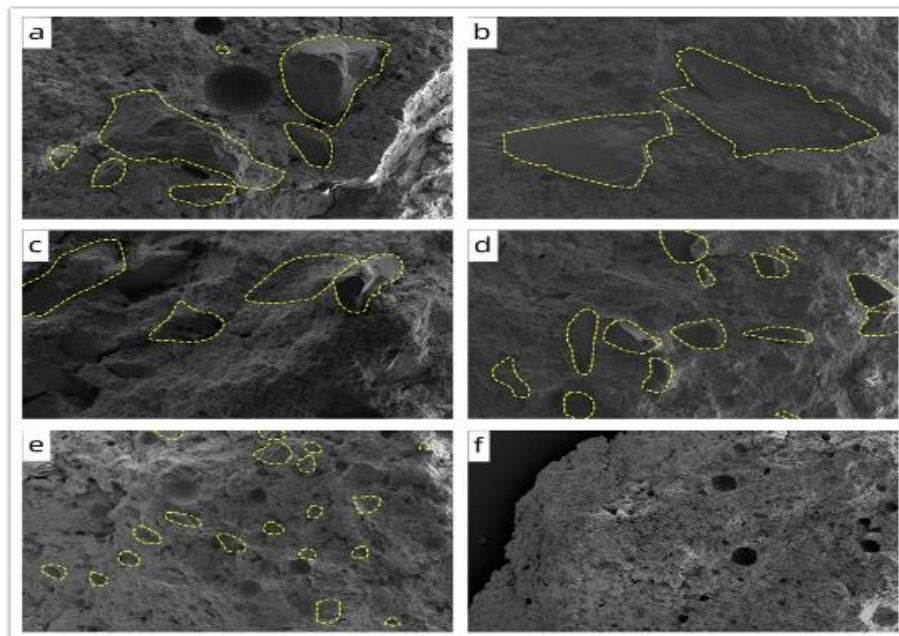


**Figure 4:** Magnified Image at 30×

Figure 4(a) shows the SEM image of sample A3 at 30× magnification, illustrating the presence of coal dust particles of varying sizes within the cement matrix, with smaller coal dust particles interspersed among larger ones. By comparing the microstructural morphology of cement-based materials with different coal dust particle sizes, it is observed that as the particle size decreases, the quantity of coal dust particles in samples B1 to B5 increases. For sample B1, the larger particle size allows for a more uniform distribution of coal dust within the cement-based material, resulting in stronger load-bearing capacity when subjected to external loads. In contrast, sample B2, with smaller particle sizes, exhibits enhanced interactions between the coal dust particles, leading to noticeable agglomeration and the formation of additional voids, which ultimately reduces the overall



compressive strength. Figure 4(b) presents the SEM image of sample B1, where larger and uniformly distributed coal dust particles can be observed, demonstrating good bonding with the cement particles, which is beneficial for improving mechanical performance. Conversely, Figures 4(c) to 4(e) illustrate the microstructures of samples B2, B3, and B4. As the particle size decreases, the distribution of coal dust particles in the cement matrix becomes increasingly uneven, resulting in a rise in porosity. Figure 4(f) displays the SEM image of sample B5, which reveals the agglomeration of fine coal dust particles, further exacerbating the internal defects of the cement-based material. This agglomeration effect significantly weakens the mechanical strength of the material. From these observations of the microstructural characteristics, it can be concluded that the selection of coal dust particle size has profound implications for the performance of cement-based materials. A well-considered particle size configuration can optimize the microstructure of the cement matrix, enhancing its compressive strength.

### XRD Experimental Results

The XRD experimental results for the hydration products of samples with varying coal dust dosages and particle sizes are presented in Figures 8 and 9.

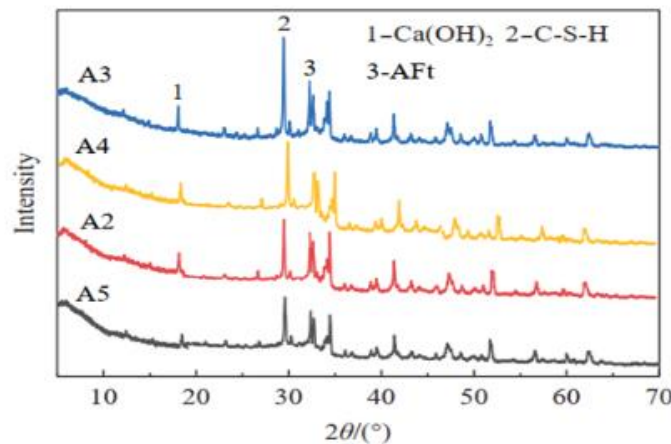


**Figure 5:** XRD Patterns of Hydration Products for Samples with Varying Coal Dust Dosages

From Figure 5, the XRD patterns indicate that the primary hydration products of the experiments are C-S-H gel, CH (calcium hydroxide), and a small amount of ettringite. The formation of these hydration products is critical to the mechanical properties of the material, particularly the C-S-H gel, which serves as the main strength contributor during cement hydration. Its content is closely related to the density and compressive strength of the material. As the dosage of coal dust increases from A2 to A3 (up to 40g), the intensity of the diffraction peaks for C-S-H gel gradually increases, suggesting a more complete hydration reaction in the cement matrix and the generation of greater amounts of C-S-H gel. This is one of the reasons why the A3 specimen exhibits the highest compressive strength. However, further increasing the coal dust dosage (as in A4 and A5) results in a decrease in the intensity of the C-S-H diffraction peaks, indicating that excessive coal dust inhibits the hydration reaction of the cement, thereby weakening the material's strength. Additionally, the diffraction peaks for CH are clearly present in all samples. The formation of CH is a byproduct of the hydration of Portland cement and does not directly contribute to strength, but its quantity can reflect the extent of cement clinker hydration. In the lower dosage samples A1 and A2, the CH peak intensity is relatively high, indicating that the hydration of the cement clinker is more complete when coal dust content is low. Conversely, as the dosage increases to A4 and A5, the peak intensity of CH gradually decreases, suggesting that the addition of coal dust has an inhibitory effect on the hydration of the cement clinker, particularly at high dosages, where the voids and agglomeration phenomena induced by the coal dust negatively impact CH formation. Furthermore, ettringite plays a significant role in promoting early hydration. XRD analysis reveals that the diffraction peaks of ettringite are pronounced in samples A1 and A2; however, as the dosage of coal dust increases, the quantity of ettringite generated gradually diminishes. This may be due to the reduced reactivity of the cement matrix when there is an excessive amount of coal dust, leading to a decrease in ettringite formation, which in turn affects the early strength of the material.



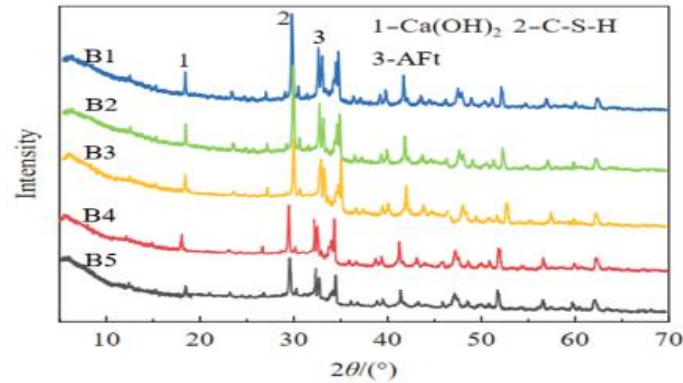


**Figure 6:** XRD Patterns of Hydration Products for Samples with Different Coal Dust Particle Sizes

As observed in Figure 9, the amount of generated C-S-H gel shows significant variation. In the sample B1 (with larger particle size coal dust), the diffraction peak of C-S-H is most prominent, indicating that the hydration reaction is most complete at this stage. As the coal dust particle size decreases (from B2 to B5), the intensity of the C-S-H peak gradually weakens, suggesting that the finer coal dust particles may adversely affect the uniform distribution of the slurry, thereby hindering the hydration reaction. Particularly in B5, the hydrophobic nature and agglomeration effects of the fine coal dust are more pronounced, leading to insufficient hydration and reduced generation of hydration products, which ultimately results in a decline in the compressive strength of the material. The variations in CH and ettringite in the different particle size samples exhibit similar trends to that of C-S-H. In sample B1, the diffraction peak of CH is more pronounced, while the amount of CH generated decreases as the particle size reduces, indicating that finer coal dust is detrimental to the hydration process of the cement-based material. The formation of ettringite is also notably significant in B1, suggesting that larger particle size coal dust is more favorable for the early hydration reaction of cement, whereas smaller particle sizes may block the pores between cement particles, thereby affecting ettringite formation.

#### 4. Conclusion

a. This study investigates the effects of coal dust dosage and particle size on the mechanical properties of cement-based grouting materials, exploring the application of coal dust as a filler in cement-based materials and providing a detailed analysis from both macro-mechanical and microstructural perspectives. The experimental results indicate that both the dosage and particle size of coal dust have a significant impact on the mechanical performance of cement-based materials. At a coal dust dosage of 40g, the material achieves its maximum compressive strength, primarily due to the formation of a dense internal structure and an increased amount of hydration products at this dosage. Excessive coal dust introduces additional pores and defects, consequently reducing the material's strength.

b. Regarding the coal dust particle size, larger particles (1–2mm) can distribute evenly within the cement matrix, enhancing the skeleton effect and improving the mechanical properties of the material. In contrast, finer coal dust particles (<0.5mm) are prone to agglomeration, affecting the uniformity and hydration reaction of the material, leading to a decrease in compressive strength. Microstructural analyses using scanning electron microscopy (SEM) and X-ray diffraction (XRD) further validate this phenomenon. The major hydration products, including C-S-H gel, CH, and ettringite, are generated in greater quantities under optimal dosage and particle size conditions, enhancing the density and strength of the material.

#### References

- [1]. Xie Heping, Wu Lixin, Zheng Dezhi. Prediction of Energy Consumption and Coal Demand in China for 2025. *Journal of Coal Science and Engineering*, 2019, 44(07): 1949-1960.
- [2]. Wang Guofa, Liu Feng, Pang Yihui, et al. Intelligent Mining: Core Technological Support for High-Quality Development of the Coal Industry. *Journal of Coal Science and Engineering*, 2019, 44(02): 349-357.



- [3]. Fu Xuehai, Zhang Xiaodong, Wei Chongtao. Research Progress on Testing, Simulation, and Prediction of Gas Content in Coal Seams. *Journal of China University of Mining & Technology*, 2021, 50(01): 13-31.
- [4]. Wang Yaofeng. Current Status and Prospects of Gas Drainage Technology and Equipment in Chinese Coal Mines. *Coal Mine Safety*, 2020, 51(10): 67-77.
- [5]. Zhang Peisen, Li Fuxing, Zhu Huicong, Niu Hui, Li Xiaohe. Statistical Analysis of Coal Mine Accidents from 2008 to 2020 and Preventive Measures. *Journal of Mining Safety and Environmental Protection*, 2022, (001): 049.
- [6]. Zhang Chaolin, Wang Enyuan, Xu Jiang, et al. Influence of Coal Seam Gas Pressure on Gas Drainage Effect. *Journal of Mining and Safety Engineering*, 2022, 39(03): 634-642.
- [7]. Li Quanxin, Xu Chao, Liu Jianlin, et al. Key Technologies and Engineering Practices for Comprehensive Gas Drainage with Directional Drilling in Coal Mines. *Journal of Coal Science and Engineering*, 2022, 47(08): 3108-3116.
- [8]. Xu Jianbing, Bai Jianmin, Hong Xiaodong. The Significance of Gas Drainage in Mines and Prevention Measures for Gas Accidents. *Inner Mongolia Coal Economy*, 2014(10): 79-80.
- [9]. Liu Jianzhong, Sun Haitao, Lei Yi, et al. Current Status and Development Trends of New Technologies for Coalbed Methane Development and Utilization in Coal Mining Areas. *Journal of Coal Science and Engineering*, 2020, 45(01): 258-267.
- [10]. Lan Zequan, Qu Rongfei, Chen Xuexi, et al. Current Status and Analysis of Direct Measurement of Coalbed Gas Pressure. *Journal of Coal Mine Safety*, 2009, 40(04): 74-78.
- [11]. Wu Hao, Zhu Meijia, Liu Zhuo, et al. Developing a polymer-based crack repairing material using interpenetrate polymer network (IPN) technology[J]. *Construction and Building Materials*, 2015,84: 192-200.
- [12]. Li Jia, Zhang Jingwei, Chen Shuo. Study on dynamic viscoelastic properties and constitutive model of non-water reacted polyurethane grouting materials[J]. *Measurement*, 2021,176: 109115.
- [13]. Wu Hailong. Research on Cement-Based Sealing Materials for Mining. *Henan Science and Technology*, 2017(11): 120-123.
- [14]. Zhang Junxiang, Sun Yuning, Sun Zhidong, et al. Analysis of Macromechanical Properties and Mechanisms of Coal Dust/Polymer Composite Grouting Materials. *Journal of Rock Mechanics and Engineering*, 2019, 38(S1): 2889-2897.
- [15]. Zhou Yang, Liang Bing, Sun Weiji, et al. Distribution Law of Drill Cuttings Particle Size with Depth in Deep Coal Seams. *Journal of Safety Science and Technology*, 2020, 16(01): 66-72.
- [16]. Knop Yaniv, Peled Alva, Cohen Ronen. Influences of limestone particle size distributions and contents on blended cement properties[J]. *Construction and Building Materials*, 2014,71: 26-34.

